

Expression of cytosolic malic enzyme (ME1) is associated with disease progression in human oral squamous cell carcinoma

Chie Nakashima^{1,2} | Kazuhiko Yamamoto² | Rina Fujiwara-Tani¹ | Yi Luo^{1,3} | Sayako Matsushima¹ | Kiyomu Fujii¹ | Hitoshi Ohmori¹ | Tomonori Sasahira¹ | Takamitsu Sasaki¹ | Yasuhiko Kitada⁴ | Tadaaki Kirita² | Hiroki Kuniyasu¹ 

¹Department of Molecular Pathology, Nara Medical University, Kashihara, Japan

²Department of Oral and Maxillofacial Surgery, Nara Medical University, Kashihara, Japan

³Jiangsu Province Key Laboratory of Neuroregeneration, Nantong University, Nantong, China

⁴Department of Health and Science, Prefectural University of Hiroshima, Hiroshima, Japan

Correspondence

Hiroki Kuniyasu, Department of Molecular Pathology, Nara Medical University, Kashihara, Japan.
Email: cooninh@zb4.so-net.ne.jp

Funding information

Ministry of Education, Culture, Sports, Science and Technology of Japan

Malic enzyme 1 (ME1) is a multifunctional protein involved in glycolysis, the citric acid cycle, NADPH production, glutamine metabolism, and lipogenesis. It is overexpressed in various cancers. We examined the expression of ME1 in 119 oral squamous cell carcinomas (OSCCs) using immunohistochemistry. Malic enzyme 1 expression was moderate to strong in 57 (48%) OSCCs and correlated with pT, pN, clinical stage, and histological grade. In 37 cases with prognostic evaluation, moderate to strong ME1 expression indicated a worse prognosis than did weak ME1 expression. Malic enzyme 1 knockdown or inactivation by lanthanide inhibited cell proliferation and motility and suppressed the epithelial-mesenchymal transition in HSC3 human OSCC cells. Knockdown of ME1 also shifted energy metabolism from aerobic glycolysis and lactate fermentation to mitochondrial oxidative phosphorylation, and the redox status from reductive to oxidative. In a mouse tumor model, lanthanide suppressed tumor growth and increased survival time. These findings reveal that ME1 is a valid target for molecular therapy in OSCC.

KEYWORDS

cancer invasion, glutamine, malic enzyme, prognosis, stemness

1 | INTRODUCTION

In the USA, approximately 2%-3% of malignant cancers are OSCCs;¹ in Japan, the percentage is approximately 1%-2%.² The frequency of OSCC is increasing worldwide,¹ and as society ages, OSCC-related morbidity and mortality rates have also increased.³ Internationally,

the OSCC incidence rate is high in countries with high tobacco use and alcohol consumption.^{4,5}

Oral squamous cell carcinoma is commonly managed with multimodal regimens consisting of surgery, radiation, and chemotherapy in various combinations.^{4,6} The 5-year survival rate for patients with oral cancer is 60%-70%. Cure rates are highest when oral cancers are treated at an early stage; conversely, late-stage oral cancers have a poor prognosis.^{7,8} Therefore, new molecular targets for effective drug treatment are needed.

When oxygen is present, most human cells convert lactate to carbon dioxide and usable energy through a mitochondria-localized process termed oxidative phosphorylation.^{9,10} The Warburg effect (ie, the rapid fermentation of glucose by tumors even in the

Abbreviations: ACC, acetyl-CoA carboxylase α ; ALP, alkaline phosphatase; EGR4, early growth response protein 4; EMT, epithelial-mesenchymal transition; G6PD, glucose-6-phosphate dehydrogenase; GLUD1, glutamate dehydrogenase 1; GSH, glutathione; GSSG, oxidized glutathione; ME1, cytoplasmic malic enzyme; MTS, 3-(4,5-dimethylthiazol-2-yl)-5-(3-carboxymethoxyphenyl)-2-(4-sulfophenyl)-2H-tetrazolium; OSCC, oral squamous cell carcinoma; PKM, pyruvate kinase M; PPAR, peroxisome proliferator-activated receptor; PPP, pentose phosphate pathway; S-ODN, S-oligodeoxynucleotide; TCA, tricarboxylic cycle.

This is an open access article under the terms of the Creative Commons Attribution-NonCommercial License, which permits use, distribution and reproduction in any medium, provided the original work is properly cited and is not used for commercial purposes.

© 2018 The Authors. *Cancer Science* published by John Wiley & Sons Australia, Ltd on behalf of Japanese Cancer Association.

presence of oxygen) was discovered by Otto Warburg.^{11,12} Most cancer cells enhance glycolysis uncoupled with oxidative phosphorylation, even though glycolysis yields lower amounts of ATP from glucose than oxidative phosphorylation.¹³

Cancer cells also often metabolize glutamine to produce enough intermediates (eg, lipids, nucleic acids, and amino acids) for construction of biological components.¹⁴ In normal human cells, glutamine is converted to α -ketoglutarate, which enters the TCA cycle. Glutamine is used for ATP production and the synthesis of nucleic acid, lipids, and other amino acids.^{15,16} Cytoplasmic ME1 decarboxylates malate to form pyruvate and ultimately NADPH.¹⁷ In cancer cells, pyruvate generated in this manner is utilized for lactate fermentation.^{18,19} Because wild-type p53 represses ME1 expression, ME1 overexpression is associated with cancers carrying mutated p53.²⁰

Epithelial-mesenchymal transition has been strongly implicated in the disease progression and poor prognosis of head and neck squamous cell carcinomas.²¹ Epithelial-mesenchymal transition is associated with decreased expression of epithelial cell-cell adhesion molecules, such as E-cadherin or claudin-4, and increased expression of mesenchymal intermediate fiber, vimentin.

In this study, we examined the role of ME1 in OSCC. Malic enzyme 1 is thought to link energy metabolism, redox status, and EMT specifically in cancer and is a putative molecular target for OSCC treatment.

2 | MATERIALS AND METHODS

2.1 | Surgical specimens

Surgical specimens from 46 primary OSCCs treated surgically at Nara Medical University Hospital (Kashihara, Japan) were randomly selected. Tumor stages and histological grades were determined by using the UICC's TNM classification system.²² The personal information of the consenting patients was anonymized by the personal information staff. All procedures were carried out in accordance with the Ethical Guidelines for Human Genome/Gene Research enacted by the Japanese Government and approved by the Ethics Committee of Nara Medical University (Approval No. 937).

2.2 | Tissue arrays

The OSCC tissue array slides were obtained from US Biomax (Rockville, MD, USA). Slides were immunostained with anti-ME1 antibody (Abnova, Taipei City, Taiwan), and the association between clinicopathological parameters and ME1 expression levels was determined.

2.3 | Immunohistochemistry

Formalin-fixed, paraffin-embedded surgical specimens were cut into 4- μ m sections. Consecutive 4- μ m sections were immunohistochemically stained by using the immunoperoxidase technique described previously.²³ The sections were incubated with 0.5 μ g/mL anti-ME1 antibody or anti-p53 antibody (DO-1; Santa-Cruz Biotechnology,

Santa Cruz, CA, USA) for 2.5 hour at room temperature. To enhance p53 immunoreactivity, the sections were boiled 3 times in a microwave oven for 15 minutes at 500 W. Secondary antibodies (Dako, Carpinteria, CA, USA) were applied for 1 hour. Tissue sections were color-developed with diaminobenzidine hydrochloride (Dako) and counterstained with Meyer's hematoxylin (Sigma Chemical, St. Louis, MO, USA). Immunoreactivity was classified as weak (score 2-3), moderate (score 4-8), or strong (score 9-12).²⁴

2.4 | Cell culture and reagents

The HSC3 cell line, which originated from a metastatic focus of a human tongue squamous cell carcinoma, was purchased from the Health Science Research Resources Bank (Osaka, Japan). HSC3 cells were maintained in DMEM containing 450 mg/dL glucose and 10% FBS in a 5% CO₂ atmosphere at 37°C. These reagents were purchased from Dako (Osaka, Japan) as were glucose-free DMEM and the ME inhibitor lanthanide (used at 1 μ mol/L).^{25,26} Mitochondria were stained with MitoGreen solution (Takara Bio, Kusatsu, Japan) and observed by fluorescence microscopy (Zeiss, Tokyo, Japan).

2.5 | Cell proliferation and cell infiltration

To assess cell proliferation, cell numbers were determined by using an autocytoometer, (CDA-1000; Sysmex, Kobe, Japan). To assess cell infiltration, wound healing assays were carried out. The cell migration area was measured on digitally captured images. In some experiments, cells received lanthanide for 48 hour at 37°C.

2.6 | Animal models

Male 5-week-old BALB/cSlc-nu/nu mice were purchased from Japan SLC (Shizuoka, Japan). The mice were maintained in accordance with the institutional guidelines approved by the Committee for Animal Experimentation of Nara Medical University and the current regulations and standards established by the Ministry of Health, Labor, and Welfare of Japan. Each experimental group contained 5 mice.

To prepare an s.c. tumor model, HSC3 cells (1×10^7 cells) suspended in Hank's balanced salt solution (Sigma Chemical) were inoculated into the scapular s.c. tissue of the mice. Lanthanide (0.5 μ mol/kg body weight in 200 μ L PBS) was injected i.p. At week 4, the tumors were excised for assessment.

2.7 | Antisense S-ODN assay

A 21-mer S-ODN antisense sequence corresponding to nucleotides 4-24 of the ME1 gene was synthesized and subsequently purified by reverse-phase HPLC (Sigma-Genosys, Ishikari, Japan). The antisense S-ODN sequence was 5'-GCG ACG GGG GGC TTC GGG CTC-3' (GenBank X77244.1). A mixed-sequence 21-mer S-ODN was used as the control. Cells were pretreated with 6 mol/L antisense or mixed S-ODN for 48 hour before additional manipulations were performed.

2.8 | Cell proliferation assays

Proliferation assays using MTS were carried out by using a Celltiter 96 Aqueous One Solution Cell Proliferation Assay kit (Promega Biosciences, San Louis Obispo, CA, USA). The plates were read on a multiscan FC microplate photometer at 490 nm. The MTS value in cells cultured with the control oligonucleotide was used as the control.

2.9 | Determination of lactate and GSH/GSSG concentrations and ALP activity

Concentrations of lactate and GSH/GSSG were determined by using a D-Lactate Assay kit (Cayman Chemical, Ann Arbor, Michigan, USA), and a GSG/GSSG Ratio Detection kit (Abcam, Cambridge, MA, USA), respectively. The ALP activity was determined by using a LabAssay ALP kit (Wako).

2.10 | Reverse transcription-PCR

Total RNA (1 µg) was used for synthesizing cDNA by using a ReverTra Ace quantitative PCR RT kit (Toyobo, Osaka, Japan). Polymerase chain reaction was carried out as specified by the provider. The PCR products were electrophoresed on 2% agarose gels and visualized by using ethidium bromide. The primer sets are listed in Table 1. Primers were synthesized by Sigma-Genosys.

2.11 | Statistical analysis

Statistical significance was assessed by using the chi square-test and Student's *t*-test with the assumption of Gaussian distribution according to the Kolmogorov and Smirnov method. Analyses were carried out by using InStat software (GraphPad, Los Angeles, CA, USA). Survival curves were calculated by using a Kaplan-Meier model (StatView 4.5; Abacus Concepts, Berkeley, CA, USA). Differences in survival times were calculated by using the Cox proportional hazard model (StatView 4.5). Statistical significance was defined as $P < .05$.

TABLE 1 Sequences of RT-PCR primers used in this study

	Forward	Reverse	GenBank accession no.
ME1	ggattgcacacctgattgtg	tcttcatgttcatgggcaaa	NM_002395.5
ECD	tgcccagaaaatgaaaaagg	gtgtatgtggcaatgcgttc	Z13009.1
CLDN4	ctccatgggctacaggtaa	agcagcgagtcgtacacctt	NM_0011305.4
SNAIL	acccacatcttctcactg	tacaaaaccacgcagaca	NM_005985.3
VIM	gagaactttgccgtgaagc	tccagcagcttctcttaggt	NM_003380.3
PKM	ctatcctctggaggctgtgc	ccagacttggtgaggacgat	BC012811.2
G6PD	gaggcctgttaccaagat	agcagtggtgaaataacg	NM_000402.4
ACC	accaccaatgccaaagtagc	ctgcaggttctcaatgcaaa	NM_198834.2
GLUD1	gaatccatggacgactctct	tccatcagactaccaaca	NM_005271.4
CD44	aagtgaggcaaacacaacc	agcttttcttctgccaca	FJ216964.1
ACTB	ggacttcgagcaagagatgg	agcactgtgtggcgtacag	NM_001101.3

3 | RESULTS

3.1 | Expression of ME1 in OSCC and relationship with p53 expression

Expression of ME1 was examined in samples from 119 cases of OSCC by immunohistochemistry (Figure 1A-F). In non-cancerous squamous epithelium, ME1 expression was barely detectable (Figure 1A). In cancerous regions (Figure 1B-F), ME1 was expressed in the cytoplasm in various patterns. Some samples showed marked intratumoral heterogeneity (Figure 1E,F).

The expression of ME1 and p53 proteins was determined by immunohistochemistry in the same histological sections. As shown by the representative data in Figure 1(G,H), ME1-positive immunoreaction was found in the cancer cells different from p53-positive cancer cells. Thus there was no relationship between p53 expression and ME1 expression in the 37 OSCCs examined.

3.2 | Relationship between ME1 expression and clinicopathological parameters in OSCC

Examination of 119 OSCCs showed that ME1 expression significantly correlated with T-factor, N-factor, and clinical stage (Table 2). As the cancers progressed, the expression of ME1 increased. In terms of histological grade, ME1 expression was higher in well-differentiated OSCCs than in OSCCs with high-grade histology.

3.3 | Relationship between ME1 expression and disease prognosis in OSCC

Although unrelated to tumor recurrence (Table 2), ME1 expression significantly correlated with the patient's prognosis (Table 3). In a follow-up study of 37 OSCC patients, 1 of 22 (5%) with ME1 weak expression died, whereas 4 of 15 (27%) with moderate to strong ME1 expression died. Mean survival time was also shorter in patients with moderate to strong ME1 expression than in those with weak ME1 expression. A survival analysis using the Kaplan-Meier method showed that patients with moderate to strong ME1 expression had significantly worse prognosis than did those with weak ME1 expression (Figure 2).

3.4 | Effect of ME1 knockdown on proliferation and ME1 inactivation on motility

Knockdown of ME1 inhibited the proliferation of HSC3 cells in medium containing 100 or 200 (but not 0 or 450) mg/dL glucose (Figure 3A). In a wound healing assay, the HSC3 cell-covered area of the wound was decreased to 38% from 85% by treatment with ME inhibitor lanthanide (Figure 3B). Lanthanide treatment inhibited invasion of HSC3 cells into a type IV collagen-coated membrane by 52% as determined in an in vitro invasion assay (Figure 3C).

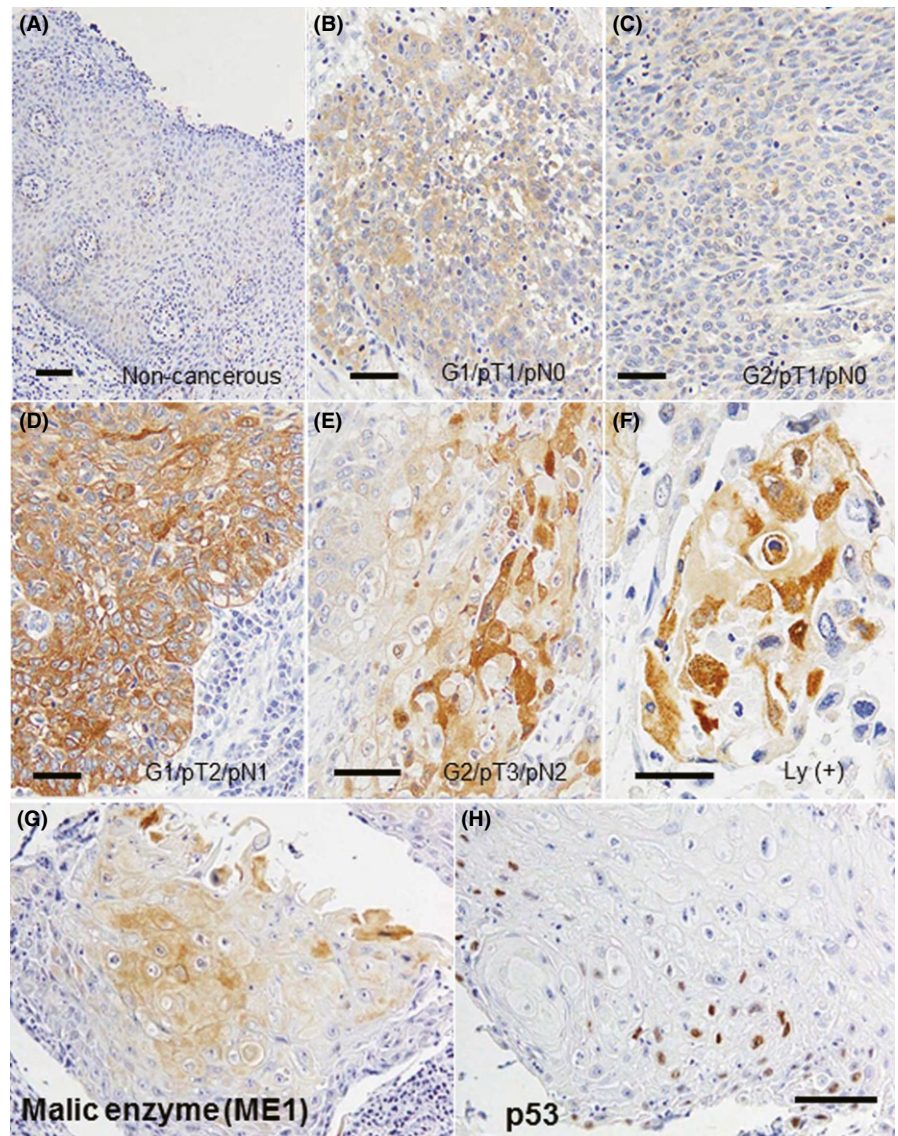


FIGURE 1 Expression of malic enzyme (ME1) in oral squamous cell carcinoma (OSCC) tissue sections. A-F, ME1 expression was determined by immunohistochemistry. A, Expression “weak” in the non-cancerous mucosa. B, Expression “moderate” in a G1/pT1/pN0 OSCC. C, Expression “weak” in a G2/pT1/pN0 OSCC. D, Expression “strong” in a G1/pT2/pN1 OSCC. E, Expression “strong” in a G2/pT3/pN2 OSCC. F, Lymphatic vessel (Ly) infiltration of the same OSCC as in panel E. (G,H) Comparison of ME1 (G) and p53 (H) expression in the same histological OSCC tissue section. Bar = 50 μm

3.5 | Effect of ME1 knockdown on the EMT and energy metabolism

Western blot analysis confirmed antisense S-ODN-mediated depletion of ME1 protein but not mitochondrial malic enzyme protein (Figure 3D). Knockdown of ME1 altered the expression of EMT-associated gene products in HSC3 cells: E-cadherin and claudin-4 mRNA levels increased, and snail and vimentin protein levels decreased (Figure 3E).

Knockdown of ME1 increased the protein levels of PKM (glycolysis), G6PD (PPP), and ACC (TCA), whereas those of GLUD1 (glutaminolysis) were not altered (Figure 3F).²⁷

3.6 | Effect of ME1 knockdown on stemness

Knockdown of ME1 suppressed (by 25%) ALP activity, which is a marker of stem cell activity²⁸ (Figure 4A). Inversely, glutamine loading (8 $\mu\text{mol/L}$) increased ALP activity (by 48%) compared to the

normal glutamine concentration (4 $\mu\text{mol/L}$). Malic enzyme 1 knockdown also decreased mRNA expression of CD44 and nanog, whereas glutamine loading increased CD44 and nanog mRNAs (Figure 4B). In Figure 4(C), protein levels of CD44, nanog, and CD133 were decreased in ME1-knockdown HSC3 cells, whereas they were increased in Avon-loaded HSC3 cells. These findings link ME1 and the glutamine metabolism to cancer cell stemness.

3.7 | Effect of ME1 knockdown on energy production

Malic enzyme 1 plays a key role in generating pyruvate from amino acids for enhanced non-mitochondrial energy production. We examined the effect of glucose and glutamine on lactate production in HSC3 cells with ME1 knockdown. Knockdown of ME1 inhibited cell proliferation and lactate production, especially in glucose-free conditions (Figure 5A). Knockdown of ME1 abrogated the promotion of growth and lactate production by glutamine addition. This finding

TABLE 2 Relationship between malic enzyme 1 (ME1) expression and clinicopathological parameters in oral squamous cell carcinoma

	ME1 expression				P-value
	Total	Weak	Moderate	Strong	
T-factor					
pT1	21	17	3	1	
pT2	56	30	16	10	
pT3-4	42	11	15	16	<.0001
N-factor					
pN0	73	49	21	3	
pN1-2	46	15	13	18	.0007
Stage					
I-II	73	44	6	6	
III-IV	46	36	15	12	.0436
Grade					
G1	54	25	11	18	
G2	41	27	10	4	
G3	24	10	10	4	.0206
Recurrence					
Negative	24	14	4	6	
Positive	13	8	3	2	NS
p53 expression					
Negative	29	19	5	5	
Positive	6	3	2	3	NS

Tumor stages and histological grades were determined according to the UICC TNM classification system.²² NS, not significant.

TABLE 3 Relationship between the expression of malic enzyme 1 (ME1) and mortality and survival time in patients with oral squamous cell carcinoma (n = 37)

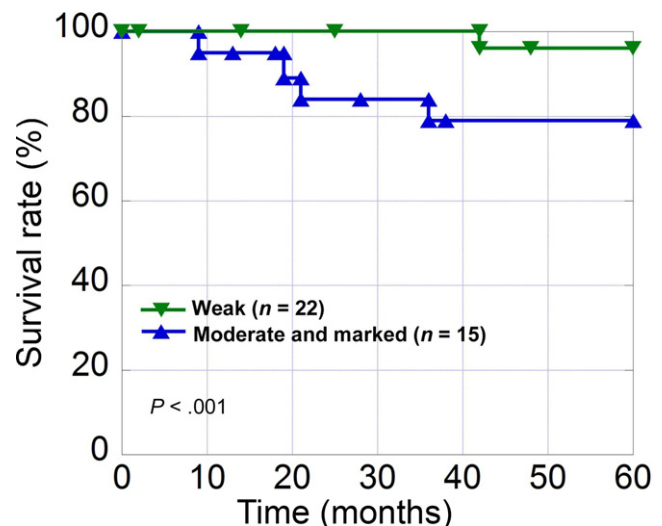
	ME1 expression		P-value
	Weak	Moderate-strong	
Mortality	1/22 (5%)	4/15 (27%)	NS
Mean survival, months	52 ± 16	37 ± 20	.0443

NS, not significant.

suggests that HSC3 cells use ME1-generated pyruvate, rather than glycolysis-generated pyruvate, for lactate fermentation in the absence of glucose. Hence, ME1 depletion might suppress pyruvate production and lactate fermentation in glucose-free conditions, in turn increasing the amount of energy generated by the TCA cycle and oxidative phosphorylation.

3.8 | Effect of ME1 knockdown on redox status

For assessing the effect of shifting energy metabolism on the redox state, we determined the GSH/GSSG ratio (GSH%) in ME1-depleted HSC3 cells (Figure 5B). The GSH% was higher when glucose was present, compared with glucose-free conditions. Knockdown of ME1

**FIGURE 2** Survival of oral squamous cell carcinoma (OSCC) patients. The overall survival rates of 37 OSCC patients were calculated by using the Kaplan-Meier method. There was a significant difference in the survival rates of patients with moderate or strong vs weak malic enzyme 1 expression ($P < .001$)

decreased the GSH% regardless of glucose concentration. Thus, ME1 knockdown enhanced the oxidative stress in HSC3 cells. Malic enzyme 1 knockdown also increased the mitochondrial area by 90% (Figure 5C).

3.9 | Effect of ME1 inactivation on tumor growth in an animal model

We finally examined the effects of ME1 inactivation on tumor growth. Lanthanide (0.5 $\mu\text{mol/kg}$ body weight, injected i.p. 8 times at 2-day intervals) suppressed tumor growth by 45% (Figure 6A). It also improved survival: the mortality rate decreased from 100% (5/5 mice) to 60% (3/5 mice) (Figure 6B), and the 50% survival period increased from 28 days to 39 days during the 40 days of observation. In Figure 6(C-G), MIB1 positivity (cell proliferation), lactate concentration, CD44 mRNA expression (stemness), and the vimentin/E-cadherin mRNA ratio (EMT) were reduced in the tumor tissue of lanthanide-treated mice compared with control mice, whereas the GSH/GSSG ratio (oxidative phosphorylation-associated oxidative stress) was increased.

4 | DISCUSSION

Malic enzyme 1, also known as cytosolic NADP⁺-dependent malic enzyme and malate dehydrogenase,²⁹ is a multifunctional protein that links the glycolytic and citric acid cycles. Interestingly, it is encoded by one of the Bach-1-targeted genes, which mediates responses to oxidative stress.³⁰ Although ME1 is important for NADPH production, glutamine metabolism, and lipogenesis,³¹ its role in cancer is unclear. Our data suggest that ME1 promotes cancer

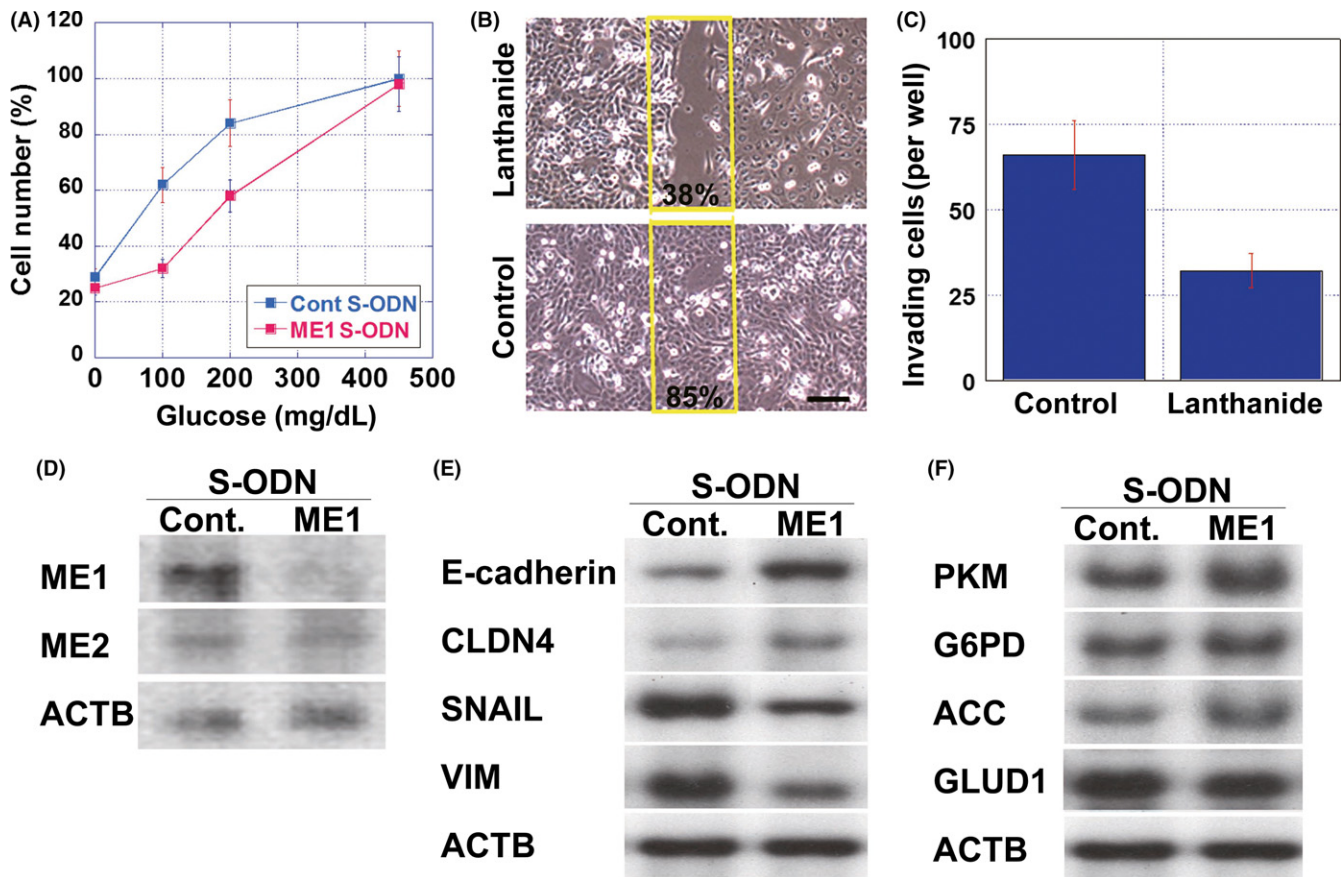


FIGURE 3 Effect of malic enzyme 1 (ME1) depletion or inactivation in HSC3 cells. A, Cell counts of cultures incubated in medium containing different concentrations of glucose after pretreatment with control (Cont) or antisense ME1 S-oligodeoxynucleotide (S-ODN). B, Wound healing assay in cells treated with the ME1 inhibitor lanthanide (1 $\mu\text{mol/L}$) for 48 hour. The yellow lines indicate the wounded area. Designated numbers were the area (%) covered with cells. Bar = 50 μm . C, Lanthanide-treated HSC3 cells were subjected to in vitro invasion assay using type IV collagen-coated insert. Numbers of invading cells into collagen membrane were measured after 48 hour. D, Western blot analysis of ME1 and mitochondrial malic enzyme (ME2) in cells treated with control (Cont.) or antisense ME1 S-ODN. E, F, Levels of epithelial-mesenchymal transition- and energy production-associated proteins were examined by Western blot. β -Actin (ACTB) served as an internal control. Error bars indicate SD (Student's *t*-test) from 3 independent experiments. ACC, acetyl-CoA carboxylase α ; CLDN4, claudin-4; G6PD, glucose-6-phosphate dehydrogenase; GLUD1, glutamate dehydrogenase 1; PKM, pyruvate kinase M; VIM, vimentin

progression by altering metabolism and stemness and subsequently increasing tumor growth and invasion. Consistent with abrogation of the EMT, ME1 depletion increased E-cadherin and claudin-4 mRNA levels and decreased SNAIL and vimentin mRNA levels in HSC3 cells. Similar results were obtained in lanthanide-treated mice with HSC3 cell-induced tumors. We also found that ME1 expression correlated with disease progression, dedifferentiation, and shorter survival times in OSCC.

Several observations suggest that ME1 is a relevant therapeutic target. First, ME1 plays a role in acquisition of EMT phenotype through the PPAR signaling pathway, which upregulates yes-associated protein and tafazzin.³² Yes-associated protein and tafazzin interacts with Snail/Slug to control stem cell function and expression of the mesenchymal phenotype.³³ Second, ME1 reduces the antitumor effects of radiation.³⁴ Third, hepatocellular carcinomas overexpressing ME1 have reduced overall and progression-free survival rates compared with those with normal ME1 levels.³¹ Finally, as

shown here, ME1 expression correlated with disease progression, dedifferentiation, and shorter survival times in OSCC.

Repression of ME1 expression by wild-type p53 has been reported, as has ME1 overexpression in cells expressing mutant p53.²⁰ Our immunohistochemical data showed no connection between the expression of these proteins in cell-based observations; however, owing to the limits of immunohistochemical analysis, p53 involvement in ME1 expression in OSCC cannot be entirely excluded. Malic enzyme 1 expression has also been linked to EMT-associated *KRAS* mutations.³¹ Mutant K-Ras upregulates ME1 in hepatocellular carcinomas³¹ and induces radiation resistance in non-small-cell lung cancers.³⁵ *KRAS*, however, is not mutated in HSC3 cells. Other regulators of ME1 expression include the canonical wnt signaling pathway in breast cancers,³⁶ a high-fat diet in the intestinal epithelium and hepatocytes,³⁷ and PPAR/EGR4.³² Although a high-fat diet and PPAR-EGR4 contribute to lipogenesis, upregulation of ME1 did not induce lipogenesis in HSC3 cells (data not shown).

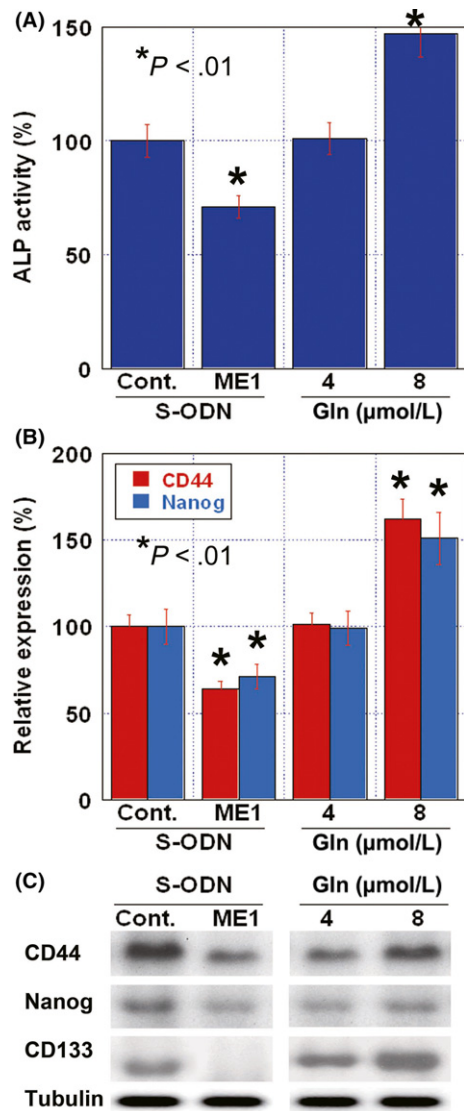


FIGURE 4 Effect of malic enzyme 1 (ME1) depletion on stemness in HSC3 cells. A, Alkaline phosphatase (ALP) activity in cells receiving control (Cont.) or antisense ME1 S-ODN or treatment with 4 or 8 $\mu\text{mol/L}$ glutamine (Gln). Error bars indicate SD (Student's *t*-test) from 3 independent experiments. B, mRNA levels of CD44 and nanog in cells treated with control (Cont.) or antisense ME1 S-ODN, or 4 or 8 $\mu\text{mol/L}$ Gln. C, Protein levels of CD44, nanog, and CD133 in CD44 mRNA in cells receiving control (Cont.) or antisense ME1 S-ODN, or 4 or 8 $\mu\text{mol/L}$ Gln. Tubulin served as an internal control

Positive feedback regulation of ME1 expression by redox status is also possible, and further investigation of the mechanisms underlying ME1 expression is warranted.

In the present study, ME1 knockdown inhibited cell proliferation, especially at low glucose and glutamine concentrations. It also upregulated the expression of PKM, G6PD, and ACC mRNA and decreased the expression of GLUT1 mRNA. As ME1 is responsible for NADPH production and the malate to pyruvate conversion, it might activate glycolysis and the PPP through a positive feedback mechanism. In support of a switch from aerobic glycolysis and

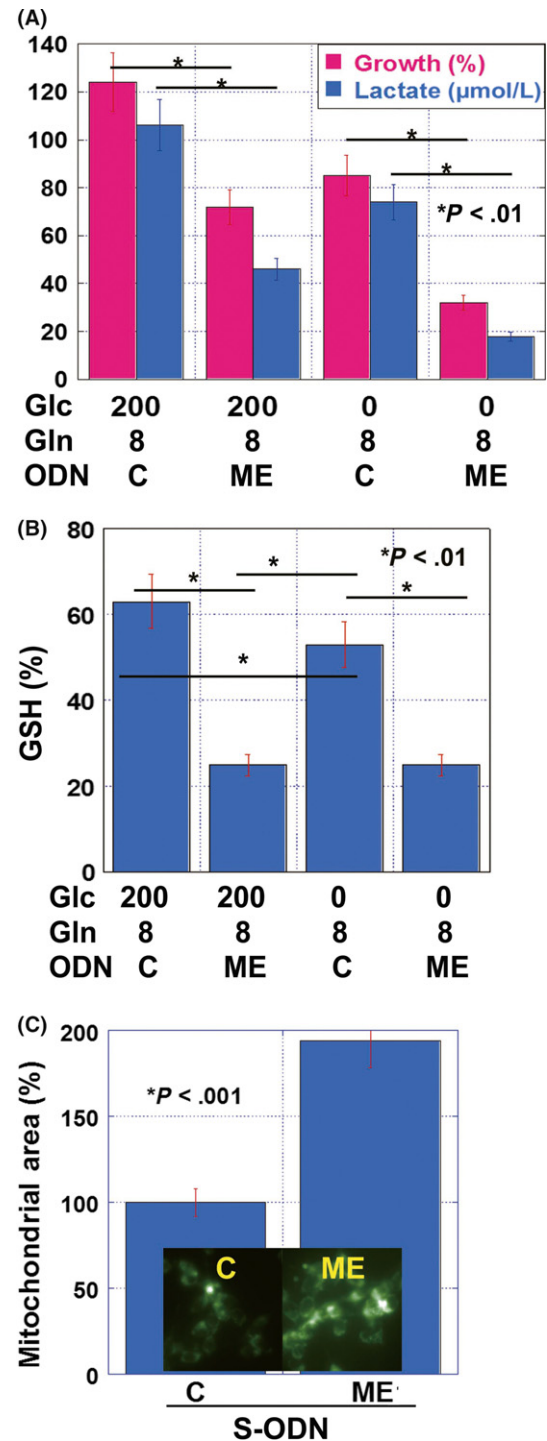


FIGURE 5 Relationship between malic enzyme 1 (ME1) expression and lactate fermentation. A, HSC3 cells were incubated in medium containing the indicated concentrations of glucose (Glc) (mg/dL) and glutamine (Gln) ($\mu\text{mol/L}$) and either control (C) or ME1 (ME) antisense S-oligonucleotide (S-ODN) (both at 6 $\mu\text{mol/L}$) for 48 hour. Cell numbers and lactate production were determined and expressed as percent control. B, Cells were treated as in panel A. The glutathione ratio (GSH%; GSH/GSH + oxidized glutathione) was determined. C, Mitochondrial area was determined by using MitoGreen in cells treated with control (C) or antisense ME1 (ME) S-ODN. Mitochondrial area is presented as the percentage of luminescence intensity. Bar = 50 $\mu\text{mol/L}$. Error bars (Student's *t*-test) show SD

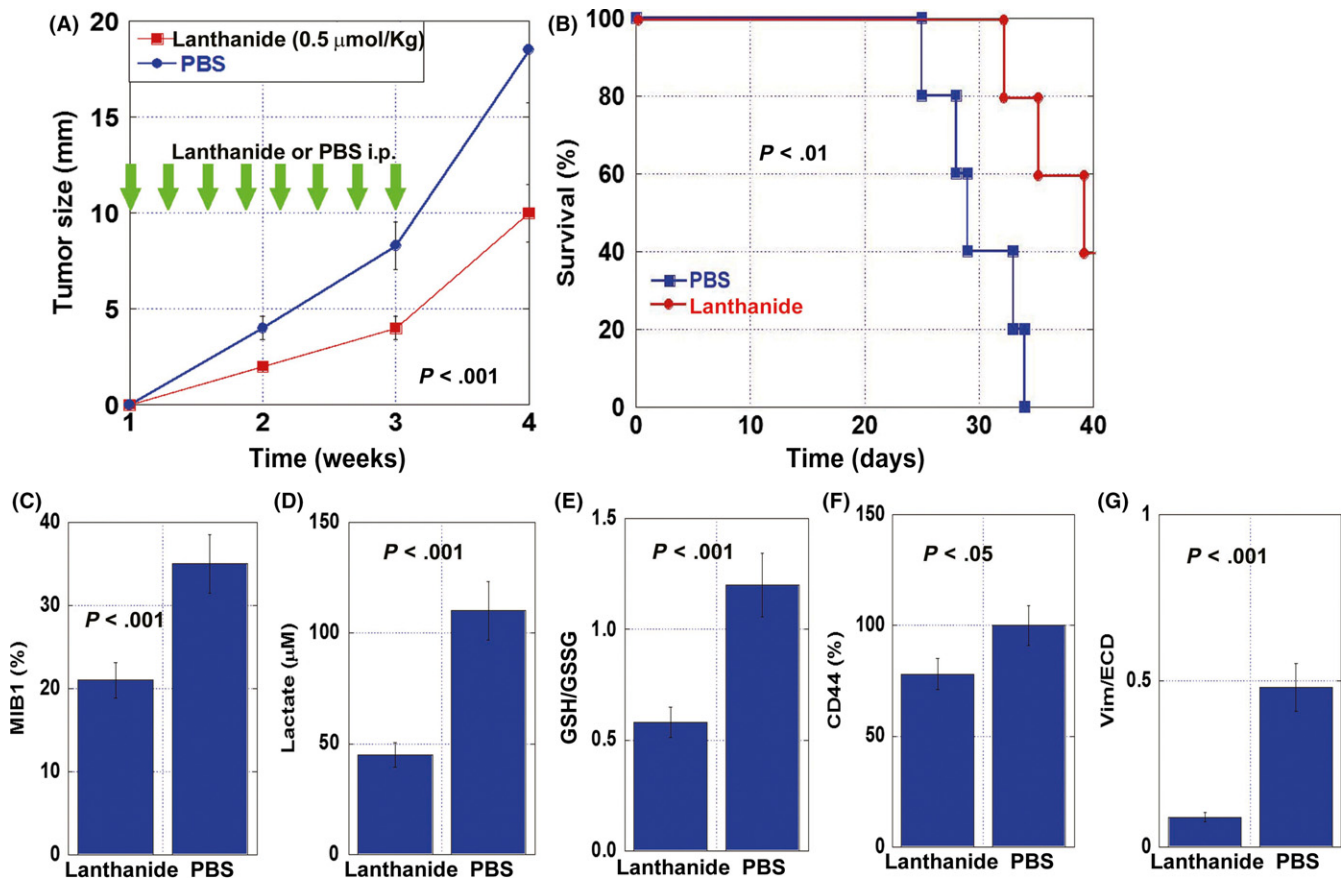


FIGURE 6 Effect of lanthanide on the growth of HSC3 cell-produced s.c. tumors in nude mice. A, Mice were inoculated with 1×10^7 HSC3 cells and i.p. injected with lanthanide (LnCl_3) ($0.5 \mu\text{mol/kg}$ body weight) or PBS (control) 8 times at 2-day intervals. Tumor diameter was measured. Each group included 5 mice. B, Mice were treated as in panel A. Survival curves were generated by using the Kaplan-Meier method. Each group included 5 mice. C-G, Mice were treated as in panel A, and the indicated parameters were measured in the tumor tissue of mice killed at week 3. C, Proliferative status was determined by MIB1 immunohistochemistry. D, Lactate fermentation was assessed by measuring lactate concentrations. E, Redox status was assessed by determining glutathione/oxidized glutathione (GSH/GSSG) ratios. F, Stemness was assessed by measuring CD44 mRNA levels. G, As an indicator of the epithelial-mesenchymal transition, the vimentin/E-cadherin mRNA ratio (Vim/ECD) was determined. Error bars (Student's *t*-test) show SD ($n = 5$)

lactate fermentation to mitochondrial oxidative phosphorylation, ME1 knockdown also increased mitochondrial area and decreased lactate production in our study. The increase of oxidative phosphorylation is thought to increase mitochondrial volume. Zheng et al³⁸ observed high glucose incorporation and PPP activity in ME1-depleted nasopharyngeal carcinoma cells, but no obvious changes in glycolysis or oxidative phosphorylation. The discrepancy between these findings and ours could reflect differences in the usage of glutamine as the energy source. In the study reported herein, lowering the glutamine concentration inhibited the proliferation of HSC3 cells, whereas raising the glutamine concentration increased the proliferative capacity of control but not ME1-depleted HSC3 cells in glucose-free medium. This observation suggests that glutamine use is upregulated in HSC3 cells and is in agreement with our previous finding of glutamine addiction in cancer cells.¹⁴

Malic enzyme 1 is involved in redox control, as confirmed by our data. Knockdown of ME1 increased the NADP/NADPH ratio and decreased the GSH/GSSG ratio in H3C3 cells, indicating that ME1 maintains a reductive state. A feedback reaction might

increase the activity of the PPP but not the glutaminolysis pathway, which would suggest that redox dysregulation is insufficiently compensated by ME1 knockdown. In previous studies, ME1 depletion decreased tolerance to low-glucose conditions³⁸ and enhanced radiation-induced growth inhibition,³⁴ largely by increasing the abundance of reactive oxygen species. The possible switching of energy production from aerobic glycolysis to oxidative phosphorylation might increase reactive oxygen species production in mitochondria.³⁹

In conclusion, our findings suggest that ME1 enhances the progression of OSCCs by increasing lactate fermentation, maintaining redox status, and promoting stemness and the EMT. The antitumor effect of ME1 inactivation in a mouse model indicates that ME1 is a relevant target for molecular therapy in OSCC.

ACKNOWLEDGMENTS

This work was supported by the Ministry of Education, Culture, Sports, Science and Technology of Japan (KAKENHI Grant Nos.

16675788 and 17831661). The authors thank Ms. Tomomi Masutani for expert assistance with the preparation of this manuscript.

CONFLICT OF INTEREST

The authors have no conflict of interest.

ORCID

Hiroki Kuniyasu  <http://orcid.org/0000-0003-2298-8825>

REFERENCES

- Siegel RL, Miller KD, Jemal A. Cancer statistics, 2016. *CA Cancer J Clin.* 2016;66:7-30.
- Wakao F, Nishimoto H, Kataonoda K, Tsukuma H, Mikami H, eds. *Cancer Statistics in Japan, 2013*. Tokyo: National Cancer Research Institute; 2013.
- Stokes WA, Fuller C, Day TA, Gillespie MB. Perioperative survival of elderly head and neck squamous cell carcinoma patients. *Laryngoscope.* 2014;124:2281-2286.
- Marur S, Forastiere AA. Head and neck squamous cell carcinoma: update on epidemiology, diagnosis, and treatment. *Mayo Clin Proc.* 2016;91:386-396.
- Warnakulasuriya S. Significant oral cancer risk associated with low socioeconomic status. *Evid Based Dent.* 2009;10:4-5.
- Ernani V, Saba NF. Oral cavity cancer: risk factors, pathology, and management. *Oncology.* 2015;89:187-195.
- Prince A, Aguirre-Ghizo J, Genden E, Posner M, Sikora A. Head and neck squamous cell carcinoma: new translational therapies. *Mt Sinai J Med.* 2010;77:684-699.
- Yao M, Epstein JB, Modi BJ, Pytynia KB, Mundt AJ, Feldman LE. Current surgical treatment of squamous cell carcinoma of the head and neck. *Oral Oncol.* 2007;43:213-223.
- Vaihteesvaran B, Xu J, Yee J, et al. The Warburg effect: a balance of flux analysis. *Metabolomics.* 2015;11:787-796.
- Icard P, Kafara P, Steyaert JM, Schwartz L, Lincet H. The metabolic cooperation between cells in solid cancer tumors. *Biochim Biophys Acta.* 2014;1846:216-225.
- Warburg O. On respiratory impairment in cancer cells. *Science.* 1956;124:269-270.
- Warburg O. On the origin of cancer cells. *Science.* 1956;123:309-314.
- Lu J, Tan M, Cai Q. The Warburg effect in tumor progression: mitochondrial oxidative metabolism as an anti-metastasis mechanism. *Cancer Lett.* 2015;356:156-164.
- Luo Y, Yoneda J, Ohmori H, et al. Cancer usurps skeletal muscle as an energy repository. *Cancer Res.* 2014;74:330-340.
- Son J, Lyssiotis CA, Ying H, et al. Glutamine supports pancreatic cancer growth through a KRAS-regulated metabolic pathway. *Nature.* 2013;496:101-105.
- Reitzer LJ, Wice BM, Kennell D. Evidence that glutamine, not sugar, is the major energy source for cultured HeLa cells. *J Biol Chem.* 1979;254:2669-2676.
- Frenkel R. Regulation and physiological functions of malic enzymes. *Curr Top Cell Regul.* 1975;9:157-181.
- Rose IA. How fumarase recycles after the malate → fumarate reaction. Insights into the reaction mechanism. *Biochemistry.* 1998;37:17651-17658.
- Wehrle JP, Ng CE, McGovern KA, et al. Metabolism of alternative substrates and the bioenergetic status of EMT6 tumor cell spheroids. *NMR Biomed.* 2000;13:349-360.
- Jiang P, Du W, Mancuso A, Wellen KE, Yang X. Reciprocal regulation of p53 and malic enzymes modulates metabolism and senescence. *Nature.* 2013;493:689-693.
- Liu JF, Mao L, Bu LL, et al. C4.4A as a biomarker of head and neck squamous cell carcinoma and correlated with epithelial mesenchymal transition. *Am J Cancer Res.* 2015;5:3505-3515.
- Sobin LH, Gospodarowicz M, Wittekind C, eds. *UICC TNM Classification of Malignant Tumours*, 7th ed. New York: John Wiley & Sons Inc; 2009.
- Kuniyasu H, Yano S, Sasaki T, Sasahira T, Sone S, Ohmori H. Colon cancer cell-derived high mobility group 1/amphoterin induces growth inhibition and apoptosis in macrophages. *Am J Pathol.* 2005;166:751-760.
- Kuniyasu H, Oue N, Wakikawa A, et al. Expression of receptors for advanced glycation end-products (RAGE) is closely associated with the invasive and metastatic activity of gastric cancer. *J Pathol.* 2002;196:163-170.
- Yoshimura E, Watanabe T. Lanthanide ions as probes in studies of metal ion-dependent enzymes. In: Sigel A, Sigel H, eds. *Metal Ions in Biological Systems - The Lanthanides and Their Interrelations With Biosystems*. Boca Raton, FL, USA: CRC Press; 2003:800.
- Yang Z, Batra R, Floyd DL, Hung H-C, Chang G-G, Tong L. Potent and competitive inhibition of malic enzymes by lanthanide ions. *Biochem Biophys Res Commun.* 2000;274:440-444.
- Grabacka MM, Wilk A, Antonczyk A, et al. Fenofibrate induces ketone body production in melanoma and Glioblastoma cells. *Front Endocrinol (Lausanne).* 2016;7:5.
- Štefková K, Procházková J, Pacherník J. Alkaline phosphatase in stem cells. *Stem Cell Int.* 2015;2015:11.
- Povey S, Wilson Jr DE, Harris H, Gormley IP, Perry P, Buckton KE. Sub-unit structure of soluble and mitochondrial malic enzyme: demonstration of human mitochondrial enzyme in human-mouse hybrids. *Ann Hum Genet.* 1975;39:203-212.
- Warnatz HJ, Schmidt D, Manke T, et al. The BTB and CNC homology 1 (BACH1) target genes are involved in the oxidative stress response and in control of the cell cycle. *J Biol Chem.* 2011;286:23521-23532.
- Wen D, Liu D, Tang J, et al. Malic enzyme 1 induces epithelial-mesenchymal transition and indicates poor prognosis in hepatocellular carcinoma. *Tumour Biol.* 2015;36:6211-6221.
- Krishnan ML, Wang Z, Silver M, et al. Possible relationship between common genetic variation and white matter development in a pilot study of preterm infants. *Brain Behav.* 2016;6:e00434.
- Tang Y, Feinberg T, Keller ET, Li XY, Weiss SJ. Snail/Slug binding interactions with YAP/TAZ control skeletal stem cell self-renewal and differentiation. *Nat Cell Biol.* 2016;18:917-929.
- Woo SH, Yang LP, Chuang HC, et al. Down-regulation of malic enzyme 1 and 2: sensitizing head and neck squamous cell carcinoma cells to therapy-induced senescence. *Head Neck.* 2016;38(Suppl 1):E934-E940.
- Chakrabarti G. Mutant KRAS associated malic enzyme 1 expression is a predictive marker for radiation therapy response in non-small cell lung cancer. *Radiat Oncol.* 2015;10:145.
- Knoblich K, Wang HX, Sharma C, Fletcher AL, Turley SJ, Hemler ME. Tetraspanin TSPAN12 regulates tumor growth and metastasis and inhibits beta-catenin degradation. *Cell Mol Life Sci.* 2014;71:1305-1314.
- Al-Dwairi A, Pabona JM, Simmen RC, Simmen FA. Cytosolic malic enzyme 1 (ME1) mediates high fat diet-induced adiposity, endocrine profile, and gastrointestinal tract proliferation-associated biomarkers in male mice. *PLoS One.* 2012;7:e46716.

38. Zheng FJ, Ye HB, Wu MS, Lian YF, Qian CN, Zeng YX. Repressing malic enzyme 1 redirects glucose metabolism, unbalances the redox state, and attenuates migratory and invasive abilities in nasopharyngeal carcinoma cell lines. *Chin J Cancer*. 2012;31:519-531.
39. Wallace DC. Mitochondria and cancer: Warburg addressed. *Cold Spring Harb Symp Quant Biol*. 2005;70:363-374.

How to cite this article: Nakashima C, Yamamoto K, Fujiwara-Tani R, et al. Expression of cytosolic malic enzyme (ME1) is associated with disease progression in human oral squamous cell carcinoma. *Cancer Sci*. 2018;109:2036-2045. <https://doi.org/10.1111/cas.13594>